Journal of Thermal Analysis and Calorimetry, Vol. 91 (2008) 1, 195–202

THERMOKINETIC STUDIES OF POLY(*o*-TOLUIDINE) DOPED WITH PERCHLORIC ACID

S. M. Ahmed[1]* *and M. I. Abd-Elrhaman*[2]

[1]Chemistry Department, Faculty of Science, Assiut University, 71516 Assiut, Egypt
[2]Physics Department, Faculty of Science, Assiut University, 71516 Assiut, Egypt

Thermokinetic parameters of the solid-state of poly(*o*-toluidine) (POT) doped with perchloric ($HClO_4$) acid was studied by thermogravimetric analysis (TG) and differential thermal analysis (DTA) under non-isothermal conditions. Molecular mechanics (MM) calculations suggest that the optimal geometric structure (OMG) of the $HClO_4$-doped POT is at least four orders of magnitude more stable than the molecular geometric (MG) structure. These calculations indicate that the potential energy (PE/kJ mol^{-1}) of the OMG is about four ($1.09\cdot10^4$) orders of magnitude lower than the MG structure of the same matrix.

The empirical formula of the doped polymer is best represented by $[\text{POT-}2HClO_4\cdot2H_2O]_n$ as substantiate by elemental analysis and MM calculations. The full polymer decomposition and degradation were found to occur in three stages during the temperature increase. The decomposition activation energy (E_d) of $HClO_4$-doped POT matrix was calculated by employing different approximations. The heating rate (α) of the decomposition and the frequency factor (K_o) were calculated. A number of equations were used to evaluate the kinetic parameters. The mechanism of the degradation of the conducting polymer is explained on the basis of their kinetic parameters. A remarkable heating rate dependence of the decomposition rate was observed.

Keywords: *DTA, elemental analyses, molecular mechanics calculations, poly(o-toluidine), thermal degradation*

Introduction

Thermally activated transformations in the solid-state can be investigated by isothermal or non-isothermal experiments [1]. In recent years conducting polymers such as polyaniline (PANI), poly(*o*-toluidine) (POT), poly(*o*-anisidine) (POAN) have attracted great attention due to their electrochemical, optical and environmental stability [2–6]. Furthermore, conducting polymers have attracted a huge amount of attention since their discovery. This is probably due to their potentiality in various applications ranging from sensor and light mass batteries to printing circuit boards in a micro-circuit technology [7–13]. Many devices need a balance of conductivity, processability and thermal stability. The difficulty in processing conducting polymers, which is one of the barriers to be conquered in a practical use, has been considerably mitigated by protonation these polymers, e.g., the protonation of polyaniline by functional organic acids and/or phenols [14–24]. The thermal stability of homo- and hetero-chain linear polymers has important applications [25–27]. Thermal degradation of *m*-nitroaniline, *m*-chloroaniline and *m*-aminophenol has been studied by Dash *et al*. [27]. In our previous work, we have found that the electrical conductivity, electroactivity, spectroelectroactivity or thermal stability could be induced into some polymeric forms [28–38].

A survey of literature reveals that the thermal degradation pattern of conducting polymers has not been seriously dealt with involving the various kinetic equations and related parameters.

In the present research, the thermal stability of $HClO_4$-doped POT matrix in solid-state have been studied using TG and DTA techniques. The decomposition kinetic parameters, such as activation energy and the frequency factor, as well as the decomposition rate were calculated to determine the decomposition mechanism of the investigated polymer.

Experimental

Materials

o-Toluidine (*o*-T) was purchased from Aldrich Chemicals Company. $HClO_4$ was received from Merck Chemicals Co. and used as received. All other chemicals used throughout this study were of analytical reagent grade of the high commercially available purity. Doubly distilled water was used in the experiments.

Poly(*o*-toluidine) doped with perchloric acid ($HClO_4$-doped POT) was prepared (in solid-state) similar to the previously described procedure [29, 34, 37].

---

* Author for correspondence: sm_ahmed@yahoo.com

1388–6150/$20.00

Akadémiai Kiadó, Budapest, Hungary
Springer, Dordrecht, The Netherlands

The chemical oxidation of *o*-toluidine (0.1 mol L^{-1}) in strong acid medium (1.0 mol L^{-1} $HClO_4$) was carried out by adding 0.2 mol L^{-1} ammonium peroxydisulfate ($(NH_4)_2S_2O_8$) solution (drop by drop). The stirring of the reaction mixture was continued for 2 h to ensure the completion of the reaction that was indicated by the stabilization of temperature of the reaction mixture. The reaction mixture was further mixed for 2–3 more h (post-polymerization) to ensure that polymerization has completed, then filtered that and washed repeatedly with distilled water and finally equilibrated in 0.1 mol L^{-1} $HClO_4$ acid which was used for 2 h to achieve maximum doping. The as-obtained polymer was dried under vacuum at 25°C to constant mass. The doped polymer was characterized by FTIR, MS spectra, elemental analysis measurement and confirmed by molecular mechanics (MM) calculations.

Instrumentation

Non-isothermal decomposition measurements, of the $HClO_4$-doped POT matrix with different heating rate (5–35 K min^{-1}), were carried out using the thermal analyst Shimadzu (DTG-60H) apparatus. The degradation was studied by using a Sartorius electrobalance (Type 2004 MP6). The sample was placed in a quartz basket suspended from the arm of the balance by means of a quartz wire. The sample temperature was adjusted using a Heraeus temperature controller (Type TRK). Elemental analyses were carried out on an Elementer analysensysteme (GmbH, Donaustr-7, 63452) Hanau, (Germany). $HClO_4$-doped POT matrix was identified in the negative-ion mode using a JMS-600 H mass spectrometer (JEOL, Tokyo, Japan) equipped with a FAB ion source and a collision cell. The fast atom helium beam was generated from He^+ ions which were accelerated to 70 V unless otherwise noted. MM calculations include MM2 and MMP2 force fields [33–38] were carried out to calculate potential energy (*PE*/kJ mol^{-1}), and dipole moment (μ/Debye) of the molecular (MG) and optimal molecular geometric (OMG) proposed structures, method normal.

Method of calculations

The energy of a molecular system is a function of the atomic coordinates and has been calculated [38] by using the following equations:

$$E(x)=E_{\mathrm{str}}+E_{\mathrm{ang}}+E_{\mathrm{stb}}+E_{\mathrm{oop}}+E_{\mathrm{tor}}+E_{\mathrm{vdw}}+E_{\mathrm{ele}}+E_{\mathrm{sol}}+E_{\mathrm{res}} \quad (1)$$

E_{str} is the bond stretch energy:

$$E_{\mathrm{str}} = w_{\mathrm{str}} \sum_{\mathrm{i-j}} k_{\mathrm{ij}} (r_{\mathrm{ij}} - L_{\mathrm{ij}})^2 + k'_{\mathrm{ij}} (r_{\mathrm{ij}} - L_{\mathrm{ij}})^3 + k''_{\mathrm{ij}} (r_{\mathrm{ij}} - L_{\mathrm{ij}})^4 \quad (2)$$

E_{ang} is the bond angle bend energy:

$$E_{\mathrm{ang}} = w_{\mathrm{ang}} \sum_{\mathrm{i-j-k}} k_{\mathrm{ijk}} d_{\mathrm{ijk}}^2 + k'_{\mathrm{ijk}} d_{\mathrm{ijk}}^3 + k''_{\mathrm{ijk}} d_{\mathrm{ijk}}^4 \quad (3)$$

E_{stb} is the stretch-bend energy:

$$E_{\mathrm{stb}} = w_{\mathrm{stb}} \sum_{\mathrm{i-j-k}} [k_{\mathrm{ijk}} (r_{\mathrm{ij}} - L_{\mathrm{ij}}) + k_{\mathrm{kji}} (r_{\mathrm{jk}} - L_{\mathrm{jk}})] d_{\mathrm{ijk}} \quad (4)$$

E_{oop} is the out-of-plane energy:

$$E_{\mathrm{oop}} = w_{\mathrm{oop}} \sum_{\mathrm{i;jkl}} k_{\mathrm{i;jkl}} X_{\mathrm{i;jkl}}^2 \quad (5)$$

E_{tor} is the torsion energy:

$$E_{\mathrm{tor}} = w_{\mathrm{tor}} \sum_{\mathrm{i-j-k-l}} \sum_{\mathrm{n-o}}^{6} k_{\mathrm{n;ijkl}} \cos(nT_{\mathrm{ijkl}} - P_{\mathrm{n;ijkl}}) \quad (6)$$

E_{vdw} is the van der Waals energy:

$$E_{\mathrm{vdw}} = w_{\mathrm{vdw}} \sum_{\mathrm{i<j}} e_{\mathrm{ij}} \left[\frac{(1+a)R_{\mathrm{ij}}}{r_{\mathrm{ij}} + aR_{\mathrm{ij}}} \right]^{\mathrm{n_{ij}}} \cdot \left[\frac{n_{\mathrm{ij}}}{\mathrm{m_{ij}}} \frac{(1+b)R_{\mathrm{ij}}^{\mathrm{m_{ij}}}}{r_{\mathrm{ij}}^{\mathrm{m_{ij}}} + bR_{\mathrm{ij}}^{\mathrm{m_{ij}}}} - \frac{m_{\mathrm{ij}} + n_{\mathrm{ij}}}{m_{\mathrm{ij}}} \right] s(r_{\mathrm{ij}}) T_{\mathrm{ij}} I_{\mathrm{ij}}^{\mathrm{vdw}} \quad (7)$$

E_{sol} is the implicit solvation energy:

$$E_{\mathrm{sol}} = -w_{\mathrm{sol}} W(d^{-1} - d_{\mathrm{x}}^{-1}) \frac{e^2}{4\pi\varepsilon_0} \cdot \frac{1}{2} \sum_{\mathrm{i-1}}^{\mathrm{n}} \sum_{\mathrm{j-1}}^{\mathrm{n}} \frac{q_{\mathrm{i}} q_{\mathrm{j}} \sqrt{G_{\mathrm{i}} G_{\mathrm{j}}}}{\sqrt{y_{\mathrm{ij}} + \exp(-y_{\mathrm{ij}})/4}} s(r_{\mathrm{ij}}) T_{\mathrm{ij}}, \quad y_{\mathrm{ij}} = r_{\mathrm{ij}}^2 G_{\mathrm{i}} G_{\mathrm{j}} \quad (8)$$

E_{ele} is the electrostatics energy:

$$E_{\mathrm{ele}} = \begin{cases} \dfrac{w_{\mathrm{ele}} e^2}{4\pi\varepsilon_0 d} \sum_{\mathrm{i<j}} q_{\mathrm{i}} q_{\mathrm{j}} \left[\dfrac{1}{r_{\mathrm{ij}} + b_{\mathrm{ele}}} \right] s(r_{\mathrm{ij}}) T_{\mathrm{ij}} I_{\mathrm{ij}}^{\mathrm{ele}} & \text{Coulomb} \\ \dfrac{w_{\mathrm{ele}} e^2}{4\pi\varepsilon_0 d} \sum_{\mathrm{i<j}} q_{\mathrm{i}} q_{\mathrm{j}} \left[\dfrac{1}{(r_{\mathrm{ij}} + b_{\mathrm{ele}})^2} \right] s(r_{\mathrm{ij}}) T_{\mathrm{ij}} I_{\mathrm{ij}}^{\mathrm{ele}} & \text{distance dependent dielectric} \\ \dfrac{w_{\mathrm{ele}} e^2}{4\pi\varepsilon_0 d} \sum_{\mathrm{i<j}} q_{\mathrm{i}} q_{\mathrm{j}} \left[\dfrac{1}{r_{\mathrm{ij}} + b_{\mathrm{ele}}} - \dfrac{\alpha r_{\mathrm{ij}}^2}{R_{\mathrm{c}}^3} - \dfrac{1-\alpha}{R_{\mathrm{c}}} \right] s(r_{\mathrm{ij}}) T_{\mathrm{ij}} I_{\mathrm{ij}}^{\mathrm{ele}} & \text{reaction field, } \alpha = \dfrac{d - d_{\mathrm{x}}}{d + 2d_{\mathrm{x}}} \end{cases} \quad (9)$$

E_{res} is the restraint energy and described as partial charges.

The amount of charge transferred at each iteration is damped with an exponentially decreasing scale factor. The amount of charge transferred between atoms *i* and *j* at each iteration when $X_i > X_j$ is:

$$dq = \frac{1}{2}\frac{X_i - X_j}{X_j^+} \tag{10}$$

where X_j^+ is the electronegativity of the positive ion of atom *j*.

Results and discussion

Elemental analysis

The elemental analysis data were compared with others for possible structures (Table 1). Calculations of the minimum error percent (%) (i.e., sum of the difference between the calculated and found percent of the elements under investigation) helped us to speculate the proposed formula as seen in Table 1. Thus the empirical formula of the doped polymer is best represented by $[POT\text{-}2HClO_4{\cdot}2H_2O]_n$ elemental analysis measurement is consisted well with the OMG structural calculations of the $POT\text{-}2HClO_4{\cdot}n/2H_2O$ chain.

MS spectra of $HClO_4$-doped POT matrix

Mass spectra (MS) were also a useful technique for the identification of $HClO_4$-doped POT matrix (Fig. 1). The intense fragment (*m*/*z*: 18) is due to the adsorbed water molecules. This result indicates that the $HClO_4$-doped POT chain have a hydrophilic nature. The hydrophilicity of this matrix has a number of possible applications including humidity determination [34]. Moreover, it has been reported that the conductivity of some conducting polymers depends strongly on the redox state, the doping level and moisture content of the polymer matrix [31, 34]. The peaks appearing at *m*/*z*: 51.61, 66.95 and 99.11, were due to ClO, ClO_2 and ClO_4, respectively, came from the dopant ($HClO_4$). The intense fragment (base peak) at *m*/*z*: 107.05 (Fig. 1) could be assignable to the $C_6H_8(CH_3)NH$, (degradation of polymer backbone) while, the signal at 180.09 is due to the $C_6H_8ClO_4$. The other fragments at higher mass (*m*/*z* 212.17, 222.13 and 303.74) could be assignable to the full-scale polymer degradation.

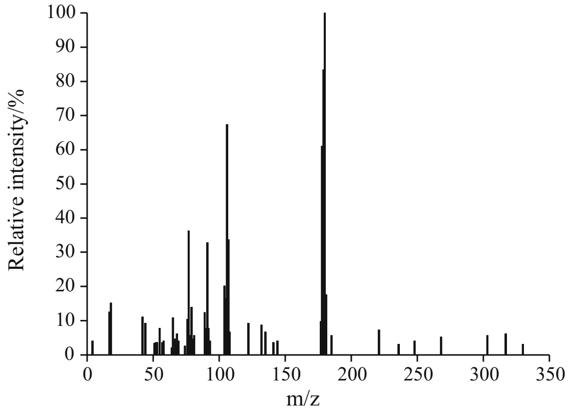

Fig. 1 Mass spectra of $HClO_4$-doped POT

Molecular mechanics calculations

MM treatment of the proposed formula was used to estimate the *PE* and dipole moment (μ) of the MG and OMG proposed structure of the polymer $[[POT\text{-}2HClO_4{\cdot}n/2H_2O]$ under investigation. It was found from these calculations that the *PE* (kJ mol^{-1}) of the MG and OMG of this matrix is equal to $8.87{\cdot}10^5$ and –81.179 kJ mol^{-1}; and μ is 6.63 and 4.68 Debye, respectively. Calculations were carried out for one repeating unit of the doped polymer chain. These calculations indicate that the *PE* and μ of the MG (Scheme 1a) is about four ($1.09{\cdot}10^4$) orders of magnitude higher than the OMG (Scheme 1b) structure of the same matrix. So, optimizing the geometry of the molecular structure (OMG) is very important for understanding the stability of this matrix. The negative value of PE and lowest dipole moment of the repeating unit indicates that the proposed geometric configuration for $[POT\text{-}2HClO_4{\cdot}2H_2O]_n$ this matrix is the most stable for this polymer.

Table 1 Speculation structure of $HClO_4$-doped POT matrix based on elemental analyses

Matrix	Element/%, calcd. (found)				
	C	H	N	Cl	min. error
$[POT\text{-}2HClO_4{\cdot}xH_2O]_n$	(50.29)	(4.90)	(8.55)	(10.35)	–
$[POT\text{-}2HClO_4{\cdot}0H_2O]_n$	54.28	4.52	9.05	11.45	32.20
$[POT\text{-}2HClO_4{\cdot}1H_2O]_n$	52.74	4.71	8.79	11.13	19.09
$[POT\text{-}2HClO_4{\cdot}2H_2O]_n$	51.29	4.88	8.54	10.82	7.05
$[POT\text{-}2HClO_4{\cdot}3H_2O]_n$	49.93	5.05	8.32	10.53	8.82
$[POT\text{-}2HClO_4{\cdot}4H_2O]_n$	48.62	5.21	8.10	10.62	15.78

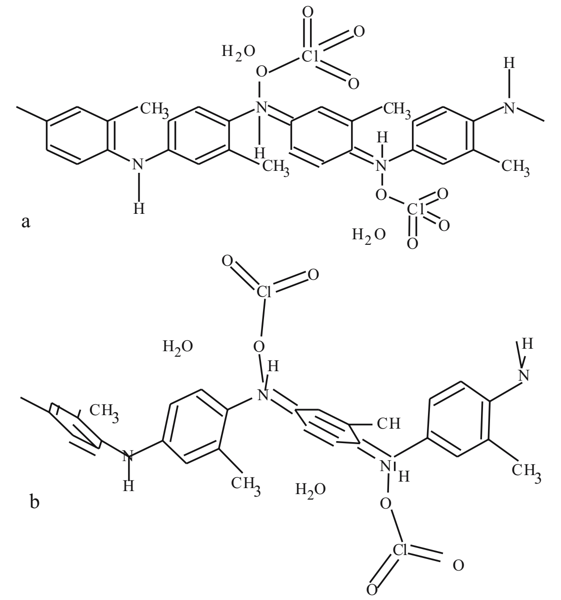

Scheme 1 a – Molecular (MG) and b – optimal molecular (OMG) geometric structure of $HClO_4$-doped POT matrix. Calculations were carried out for tetramer form (repeating unit) of POT chain, using MM calculations

Thermogravimetric analyses of $HClO_4$-doped POT matrix

TG of the doped polymer ($HClO_4$-doped POT) matrix was carried out at different heating rates as shown in Fig. 2. The doped polymer shows a three steps mass loss (Table 2) which is similar to the homoplymers of polyaniline and poly(toluidine) [39]. The initial mass loss between 313 and 393 K could be attributed to the loss of moisture, volatilization of the solvent. The proportion of moisture increases with increasing the heating rate as seen in Table 2. The second step occurring between 393 and 603 K is due to the loss of the dopant ($HClO_4$). The higher mass loss of this step is about 24% at lower heating rate (5 K min^{-1}). This observation indicates that dedoping is faster at lower heating than at higher heating rate. So there are two factors controlling the thermal stability of the doped polymer which are: (*i*) temperature dependent and (*ii*) heating rate. The decomposition pattern between 623 and 773 K is due to the degradation of the POT backbone.

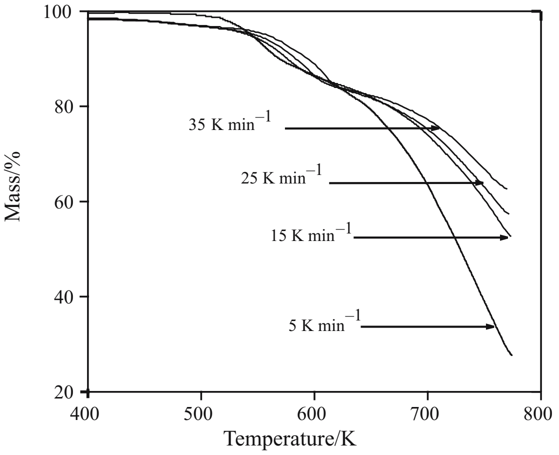

Fig. 2 TG of POT-doped with $HClO_4$ at different heating rates

Differential thermal analysis

Figure 3 shows the differential thermal analyses (DTA) curves of the $HClO_4$-doped POT polymer under the non-isothermal conditions, taken at different heating rates (α) (5, 15, 25 and 35 K min^{-1}). Each DTA trace has an exothermic peak corresponding to the peak temperature of decomposition (T_d). On the basis of the DTA results, it was clear that T_d shifted to higher temperature as the heating rate (α) was increased. The value T_d was shifted from 559 to 610 K when α was changed from 5 to 35 K min^{-1}. This means that the thermal stability of doped POT is highly dependent on the heating rate. The decomposition of the dedoped POT chain has been reported [40] to occur in the temperature range from 663 to 734 K as evidenced by DSC experiment. This indicates that the emeraldine base form (POT-EB) is thermally

Table 2 Influence of heating rate (K min^{-1}) on the mass loss of POT-doped $HClO_4$

Heating rate/K min^{-1}	Temperature range/K	mass loss	
		mg	%
5	40–120	0.025	0.55
	120–330	1.585	24.10
	330–500	2.133	48.86
15	40–120	0.062	1.35
	120–330	0.629	14.37
	330–500	1.303	28.41
25	40–120	0.067	1.46
	120–330	0.571	15.65
	330–500	1.004	21.95
35	40–120	0.074	1.63
	120–330	0.603	13.25
	330–500	0.969	21.13

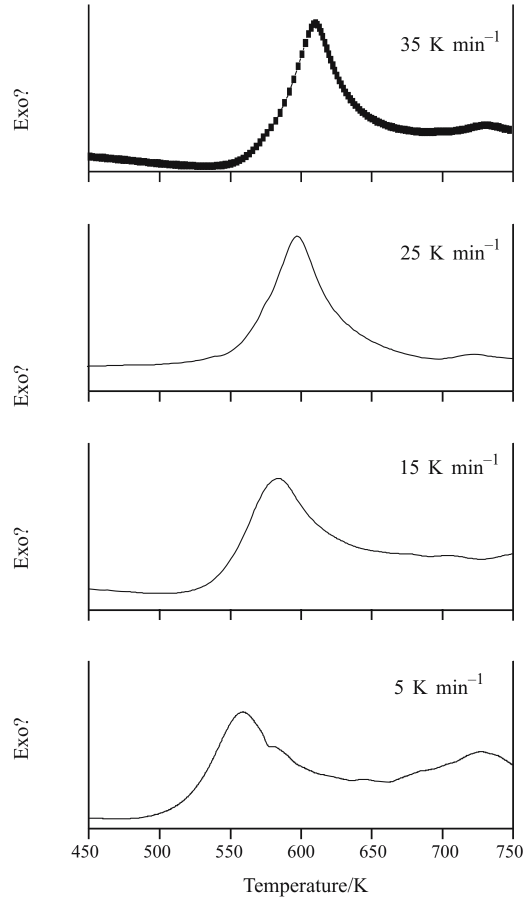

Fig. 3 Typical DTA traces of POT-doped with $HClO_4$ at different heating rates

more stable than the $HClO_4$-doped POT matrix. The exothermic peak at about 610 K (α=35 K min^{-1}) suggests that the interchain crosslinking and thermally effected morphological changes take place [41–44]. The curve also confirms that the absence of any glass transition (T_g) or melting (T_m) states for the $HClO_4$-doped POT chain and is in good agreement with the literature [45].

The decomposition activation energy (E_d) of this polymer can be calculated using the equation proposed by Chen [46]:

$$\ln\left(\frac{\alpha}{T}\right) = -\frac{E}{R}\frac{1}{T} + \ln k_0 \qquad (11)$$

where R is the gas constant and k_0 is the frequency factor. This equation is used specifically for non-isothermal crystallization [46]. It can be applied here to obtain the decomposition kinetics of the $HClO_4$-doped POT chain. This equation was successfully applied in our previous work to understand the decomposition kinetics of the derivatives of the tetrahydro-thiadiazine-2-thione [47]. By utilizing the successive approximation method, the approximate activation energies have been determined [48, 49]. The constant in Eq. (12) may be easily recalculated and the correct activation energies can be obtained. For $20 \le E/RT \le 60$, the slopes that average to 0.457 were used in Eq. (12).

$$\frac{d(\ln\alpha)}{d(1/T)} = \frac{0.457}{R}E \qquad (12)$$

where E represents the activation energy describing the overall decomposition process, E_d and T_p depicts the decomposition peak temperature, T_d. The relation between $\ln(\alpha/T_d)$ and $(1/T_d)$ obtained from the curves of the studied polymer is linear and indicates the validity of this relationship (Fig. 4). The decomposition activation energy was calculated from the slope of the line fitted to the experimental data to be 229.50 kJ mol^{-1}. The decomposition activation energy of polyaniline (N-ethyl PANI) and that of the N-ethyl PANI doped with camphorsulfonic acid (CSA) have been obtained to be 335 and 190 kJ mol^{-1}, respectively [49]. This indicates that POT-$HClO_4$ is thermally less stable than the undoped polyaniline and more thermally stable than that doped with CSA.

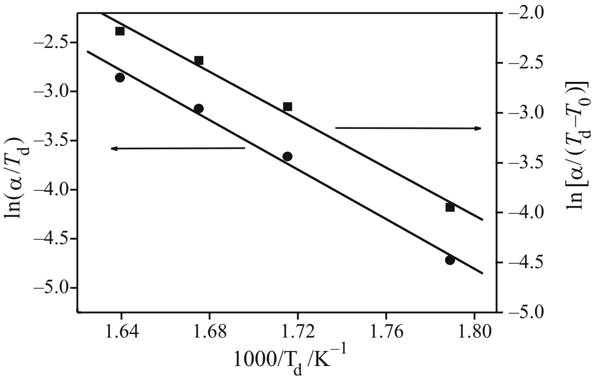

Fig. 4 Plots of $\ln(\alpha/T_d)$ and $\ln[\alpha/(T_d–T_0)]$ *vs.* $(1/T_d)$ of $HClO_4$-doped POT

The constant k_0 as decomposition parameter, measures the probability of molecular decomposes effective for the diffuse of the activated complexes. It was calculated from the intercept of the straight fitting line with vertical axis (Eq. (11)) and was found to be $5.941\cdot10^7\pm4.26$ s^{-1}.

The heat of fusion or enthalpy (ΔH), as a thermodynamic parameter, may be considered as the heat required to increase the interatomic or intermolecular distance in the complexes ($HClO_4$-doped POT), thus allowing melting or decomposition to occur. Complexes that are bound together by weak forces generally have a low heat of fusion and low melting or decomposition point. On the other hand, strong bounding forces have a higher decomposition temperature. The enthalpy of the investigated polymer was obtained from the computer program involved in the DTA apparatus and found to be $1.76\cdot10^3$ kJ kg^{-1} at heating rate

Table 3 Influence of heating rate (K min^{-1}) on the heat of fusion (ΔH) of $HClO_4$-doped POT

Heating rate/ K min^{-1}	Temperature peak, T_p/°C	ΔH/ J	ΔH/ kJ g^{-1}
5	285.75	6.39	1.40
15	310.43	8.07	1.76
25	324.15	8.10	1.77
35	337.07	1.43	$3.15\cdot10^{-2}$

of 15 K min^{-1} (Table 3). The value of ΔH usually increases with the length of the chain. It has been found to be $2.13\cdot10^3$ kJ kg^{-1} for the PANI at the same heating rate [50]. That means that the doped POT is thermally less stable than PANI. The reason may be the methylene *o*-substituted in POT chain. Usually, functionalized organic acids such as CSA, DBSA, picric acid doped polyaniline or some derivatives thermally unstable than the mineral acids [28, 37].

When E/RT>>1, a modification of Eq. (11) by Augis and Bennet [51] in the following form

$$\frac{\mathrm{d}(\ln\alpha)}{\mathrm{d}[1/(T_\mathrm{d}-T_0)]}=-\frac{0.457}{R}E_\mathrm{d} \tag{13}$$

can also be used to determine the decomposition activation energy, where T_0 is the room temperature. The plot of $\ln[(\alpha/(T_d-T_0)]$ *vs.* $1/T_d$ gives the value of E_d. Figure 4 shows a linear fit using the Eq. (13) to the experimental data yielding the value of E_d from the slope to be 218.29 kJ mol^{-1} as seen in Table 4.

The interpretation of DTA data is provided by the formal theory of transformation kinetics as the decomposition rate constant (K) is usually assumed to be an Arrhenian temperature dependence

$$K=k_0\exp(-E_d/RT) \tag{14}$$

where T is any temperature in the entire region of exothermic peak. The constant K describes the decomposition rate at any temperature, T. Substituting the obtained values of E_d and k_0 from Eqs (11) and (12), one can calculate K as a function of T for each heating rate. The calculated values of $K(T)$ at different heating rates were plotted as ln$K$ *vs.* $1/T$ and the straight lines were shown in Fig. 5. The validity of Eq. (14) for each heating rate confirms the results obtained for E_d and k_0. Figure 4 shows a remarkable heating rate dependence of the decomposition rate.

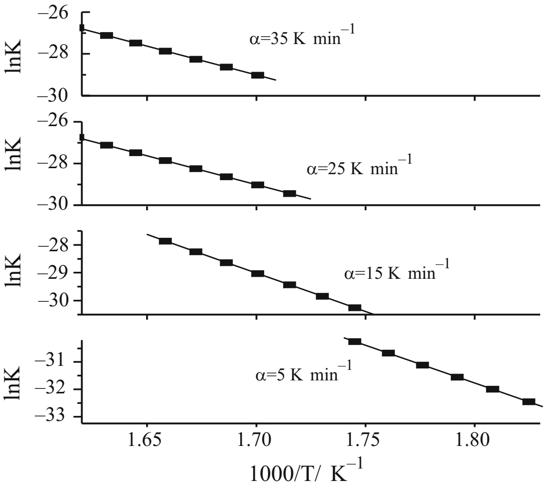

Fig. 5 Temperature dependence of the decomposition rate constant for $HClO_4$-doped. POT at different heating rates

The value of E_d of a complex can also be calculated by using a method suggested by Kissinger [52]. According to this method, the temperature of the exothermic peak depends on the heating rate by the following relation

$$\ln\frac{\alpha}{T^2}=-\frac{0.457E}{R}\frac{1}{T}+\mathrm{constant} \tag{15}$$

where E is the activation energy of the crystallization. This expression is usually used to model the crystallization kinetics in materials having amorphous-crystalline transformation. However, it is possible to use this expression to study the decomposition kinetics of materials which undergo thermal degradation [53]. In this case, E_d and T_d replace E and T. Based on Eq. (15), plotting of $\ln(\alpha/T_d^2)$ *vs.* $(1/T_d)$ gives a linear relation. The experimental points show a good fit with above relation, as shown in Fig. 5. The decomposition activation energy of the investigated polymer was determined from the straight lines and was found to be equal 215.49 kJ mol^{-1}. The obtained value of E_d by Eq. (15) is close to that got from Eq. (13), indicating eligibility of both equations in deriving the decomposition kinetics of the studied polymer.

The decomposition activation energy, E_d, can also be calculated by using the Mahadevan *et al.* ap-

Table 4 Decomposition activation energy (E_d) of $HClO_4$-doped POT using different methods

Method	Equation	Variable *vs.* $1/T_d$	Activation energy/kJ mol^{-1}
Chen	(12)	$\ln(\alpha/T_d)$	229.50±0.05
Angis and Bennet	(13)	$\ln[\alpha/(T_d-T_0)]$	218.29±0.84
Kissinger	(15)	$\ln(\alpha/T_d^2)$	215.49±1.00
Mahadevan *et al.*	(16)	$\ln\alpha$	240.15±0.84

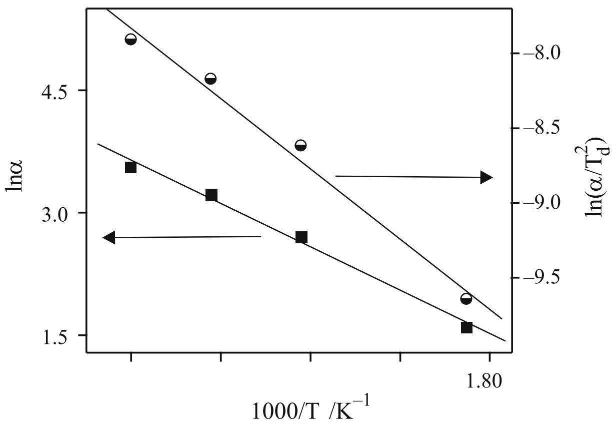

Fig. 6 Plots of ln(α)*s* *vs.* ($1/T_d$) for the $HClO_4$-doped POT

proximation [54]. The variation of $\ln(\alpha / T_d^2)$ with lnα is much slower than that of ($1/T_d$) *vs.* lnα. Thus, the Kissinger equation can be rewritten in the form of Mahadevan *et al.* [54] approximation as follows:

$$\ln\alpha = -\frac{0.457E}{R}\frac{1}{T} + \text{constant} \qquad (16)$$

Straight lines due to the plots of ($1/T_d$) *vs.* lnα were shown in Fig. 6 indicating the legality of this equation. The values of E_d was deduced from the slope of the fitting line and given in Table 2. The results in this table show that the error due to the fitting of Eq. (1) to the experimental data are much smaller than those due to the fitting using other equations. Thus, one can conclude that the approximation suggested by Chen [46] is more suitable in determining the E_d value and in describing the decomposition mechanism than other expressions.

Conclusions

Elemental analyses and the negative value of PE of the OMG structure for $[POT\text{-}2HClO_4{\cdot}2H_2O]_n$ indicate that this matrix is the highly stable. Thermal degradation of poly(*o*-toluidine) doped with perchloric acid occurs in three stages, each relating to a loss in mass. These stages involve the removal of adsorbed (moisture) water or solvent, the second stage is due to the loss of dopant and the third step could be attributed to the full polymer degradation. The decomposition parameters, E_d and k_0, were determined using the results of the differential thermal analysis. The decomposition rate was strongly dependent on the heating rate. The methods used to evaluate the decomposition activation energy were valid to describe the decomposition mechanism.

References

1 N. Rysava, T. Spasov and L. Tichy, J. Thermal Anal., 32 (1987) 1015.
2 A. G. MacDiarmid, S. L Mu, N. L. D. Somasiri and W. Wu, Mol. Cryst. Liq. Cryst., 121 (1985) 187.
3 M. C. Gupta and S. S. Umare, Macromolecules, 25 (1992) 138.
4 T. Nakayima and T. Kawagoe, Synth. Met., 28 (1989) E-696.
5 P. Hany, C. E. Santier and M. Genies, J. Appl. Electrochem., 18 (1989) 751.
6 P. Hany,C. Santier and E. M. Genies, Synth. Met., 3 (1989) 369.
7 M. C. Gupta and A. D. Borker, Indian J. Chem., 29A (1990) 631.
8 K. Ogura, H. Shiigi, M. Nakayama and A. Fujii, Electrochem. Soc., 145 (1998) 3351.
9 B. Wessling, Synth. Met., 93 (1998) 143.
10 Y. Cao, G. M. Treacy, P. Smith and A. J. Heeger, Appl. Phys. Lett., 60 (1992) 2711.
11 A. Tsumura, H. Koezuka and T. Ando, Appl. Phys. Lett., 49 (1986) 1210.
12 C. T. Kuo, A. S. Chen, G. W. Hwang and H. H. Kuo, Synth. Met., 93 (1998) 155.
13 J. H. Burroughes, D. D. C. Bradley, A. R. Brown, R. N. Marks, K. Mackay, R. H. Friend, P. L. Burn and A. B. Holmes, Nature, 347 (1990) 539.
14 Y. Cao, P. Smith and A. J. Heeger, Synth. Met., 55–57 (1993) 3514.
15 B. Sanjai, A. Raghunathan, T. S. Natarajan and G. Raangaraijan, Phys. Rev. B, 55 (1991) 10734.
16 E. R. Holland, S. J. Pomfert, P. N. Adams and A. P. Monkman, J. Phys.: Condens. Matter, 8 (1996) 2991.
17 A. P. Monkman, E. Rebourt and A. Petr, Synth. Met., 84 (1997).
18 Y. Cao, J. Qui and P. Smith, Synth. Met., 69 (1993) 187.
19 S. S. Goh, H. S. O. Chan and C. H. Ong, Polymer, 37 (1996) 2675.
20 Y. Z. Wang, J. Joo, C. H. Hsu and A. J. Epstein, Synth. Met., 68 (1995) 207.
21 A. G. MacDiarmid and A. J. Epstein, Synth. Met., 65 (1994) 103.
22 Z. H. Wang, A. Ray, A. G. MacDiarmid and A. J. Epstein, Phys. Rev. B, 43 (1991) 4373.
23 H. Varela and R. M. Torresi, J. Electrochem. Soc., 147 (2000) 665.
24 J. Stejskal, I. Sapurina, M. Trchova, J. Prokes, I. Krivka and E. Tobolkova, Macromolecules, 31 (1998) 2218.
25 R. H. Boyd, Thermal Stability of Polymers, R. T. Conley, Ed., Marcel Dekker, New York 1970, pp. 47–89.
26 A. Inaba and T. Kashiwagi, Macromolecules, 19 (1986) 2412.
27 D. K. Dash, S. K. Sahu and P. L. Nayak, J. Therm. Anal. Cal., 86 (2006) 517.
28 S. M. Ahmed, Eur. Polym. J., 38 (2002) 25.
29 R. C. Patil, S. M. Ahmed and K. Ogura, Polym. J., 33 (2000) 466.
30 T. Nagaoka, S. M. Ahmed and K. Ogura, J. Electrochem. Soc., 146 (1999) 3378.
31 R. C. Patil, S. M. Ahmed, H. Shiigi, M. Nakayama and K. Ogura, Polym. Sci. Part A: Polym. Chem., 37 (1999) 4596.

32 S. M. Ahmed, T. Nagaoka and K. Ogura, Anal. Sci., 14 (1998) 535.
33 S. M. Ahmed, Polym. Degrad. Stab., 85 (2004) 605.
34 S. M. Ahmed, J. Int J. Chem. Kinet., 35 (2003) 260.
35 M. M Kamal, S. M. Ahmed, M. M. Shahata and Y. M. Temerk, Anal. Bioanal. Chem., 372 (2002) 843.
36 S. M. Ahmed, M. M. Shahata and M. Kamal, Inorg. Organomet. Polym., 13 (2003) 171.
37 S. M. Ahmed, B. M. Abu-Zied, J. Anal. Appl. Pyrolysis, 70 (2003) 277.
38 U. Burkert and N. L. Allinger, Molecular Mechanics, ACS Monograph, 177, American Chemical Society, Washington, DC 1982.
39 P. Savitha and D. N. Sathyanarayana, Synth. Met., 154 (2004) 113.
40 C. Civakumar, T. C. Wen, A. Gopalan and H. Teng, Synth. Met., 123 (2003) 219.
41 W. Shenglong, W. Fosong and G. Xiaohui, Synth. Met., 79 (1986) 11.
42 A. L. Sharma, V. Saxena, S. Annapoorni and B. D. Malhotra, J. Appl. Polym. Sci., 81 (2001) 1460.
43 Y. Wei, G. W. Tang, K. F. Husch, E. M. Sherr, A. G. MacDiarmid and A. J. Epstein, Polymer, 33 (1992) 314.
44 H. S. O. Chan, S. C. Ng, W. S. Sim, W. S. H. Seo and B. T. G. Tan, Macromolecules, 26 (1993) 144.
45 M. V. Kulkarni, A. K. Viswanath and U. P. Mulik, Mater. Chem. Phys., 89 (2005) 1.
46 H. S. Chen, J. Non-Cryst. Solids, 27 (1978) 227.
47 M. I. Abd-Elrahman, M. O. Ahmed, S. M. Ahmed, T. Aboul-Fadl and A. El-Shorbagi, Biophys. Chem., 97 (2002) 113.
48 J. H. Flynn and L. A. Wall, Polym. Lett., 4 (1989) 323.
49 F. Cataldo and P. Maltese, Eur. Polym. J., 38 (2002) 1791.
50 S. Kazim, V. Ali, M. Zulfequar, M. Mazharul Haq and M. Husain, Current Appl. Phys., (2006) Elsevier, in press.
51 J. A. Augis and J. E. Bennent, J. Electrochem. Soc., 125 (1978) 330.
52 H. G. Kissinger, Anal. Chem., 29 (1957) 1702.
53 S. Niazi, J. Pharm. Sci., 67 (1978) 488.
54 S. Mahadevan, A. Giridhar and A. K. Singh, J. Non-Cryst. Solids, 88 (1986) 11.

Received: January 30, 2007
Accepted: April 3, 2007
OnlineFirst: July 11, 2007

DOI: 10.1007/s10973-007-8364-5